


Nociceptor Neurons are Involved in the Host Response to *Escherichia coli* Urinary Tract Infections

Zhengdong Gao^{1,2,*}, Yaxiao Liu^{1,2,*}, Lekai Zhang^{1,2}, Zizhuo Yang^{1,2}, Linchen Lv^{1,2}, Shuai Wang^{1,2}, Lipeng Chen^{1,2}, Nan Zhou^{1,2}, Yaofeng Zhu¹, Xuewen Jiang¹, Benkang Shi^{1,2}, Yan Li^{1,2} 

¹Department of Urology, Qilu Hospital of Shandong University, Jinan, People's Republic of China; ²Key Laboratory of Urinary Precision Diagnosis and Treatment in Universities of Shandong, Jinan, People's Republic of China

*These authors contributed equally to this work

Correspondence: Benkang Shi; Yan Li, Department of Urology, Qilu Hospital of Shandong University, 107 Wenhuxi Road, Jinan, 250012, People's Republic of China, Email bkang68@sdu.edu.cn; yanli@sdu.edu.cn

Purpose: Urinary tract infections (UTIs) can evoke a rapid host immune response leading to bladder inflammation and epithelial damage. Neuroimmune interactions are critical for regulating immune function in mucosal tissues. Yet the role of nociceptor neurons in bladder host defense has not been well defined. This study aimed to explore the interaction between nociceptor neurons and bladder immune system during UTIs.

Methods: In this study, whether uropathogenic *Escherichia coli* (UPEC) and lipopolysaccharide (LPS) can directly stimulate nociceptor neurons was detected. Female C57BL/6J mice were treated with high dose of capsaicin, a high-affinity TRPV1 agonist, to ablate nociceptor neurons. Bladder inflammation, barrier epithelial function and bladder immune cell infiltration were assessed after UPEC infection. The level of neuropeptide calcitonin gene-related peptide (CGRP) in infected bladder was detected. Furthermore, the effects of CGRP on neutrophils and macrophages were evaluated both in vitro and in vivo.

Results: We found that UPEC and its pathogenic factor LPS could directly excite nociceptor neurons, releasing CGRP into infected bladder, which suppressed the recruitment of neutrophils, the polarization of macrophages and the killing function of UPEC. Both Botulinum neurotoxin A (BoNT/A) and BIBN4096 (CGRP antagonism) blocked neuronal inhibition and prevented against UPEC infection.

Conclusion: The present study showed a novel mechanism by which UPEC stimulated the secretion of CGRP from nociceptor neurons to suppress innate immunity.

Keywords: UTIs, CGRP, nociceptor neurons, UPEC, innate immune cells

Introduction

Urinary tract infections (UTIs) are one of the most common bacterial infections, infecting >150 million people per year.¹ Most of UTIs are caused by uropathogenic *Escherichia coli* (UPEC).^{2,3} Bacterial infection evokes strong host responses of bladder, releasing powerful cytokines and recruiting extensive neutrophils and macrophages into the bladder.⁴⁻⁷ The host response of bladder also induces a large area of bladder superficial epithelium to fall off, which is regarded as a defense mechanism to reduce the infecting bacterial load.^{8,9} Despite the strong host response to bacteria, the urinary tract is highly vulnerable to infection and the incidence of infection recurrence is also very high. Clinically, UPECs are resistant to many antibiotics.¹⁰ Until now, there are still many unknowns about the regulating mechanism of host responses to UTIs. The underlying reasons for the insufficient host response to bacterial infection are unclear.

The urinary tract is one of the most abundantly innervated tissues and possesses complex afferent and efferent reflex pathways.¹¹ Nociceptors are sensory neurons that protect organisms from dangers by evoking pain.¹² In addition to signaling pain, it is increasingly clear that nociceptor sensory neurons are closely associated with the function of immune system in response to infection.¹³ It has been found that nociceptor neurons can modulate the function of macrophages, neutrophils, T cells and dendritic cells by altering gene expression, cytokine production, immune cell recruitment and immunophenotypic change.¹³ Specifically, *S. pyogenes* stimulate nociceptor neurons releasing CGRP, which suppresses neutrophils recruitment and bactericidal activity, thereby enhancing *S. pyogenes* survival in the skin.¹⁴ In *S. aureus* skin infection, activation of nociceptor neurons decreases TNF- α production from macrophages.¹⁵ In the lung, activation of nociceptor neurons limits neutrophils and $\gamma\delta$ T cells in *Staphylococcus aureus* infection, and this effect is mainly mediated by CGRP.¹⁶ By contrast, nociceptor neurons affect IL-23 production from CD301b⁺ dermal dendritic cells and IL-17a production from $\gamma\delta$ T cells to promote the clearance of skin *C. albicans*.¹⁷ These recent studies demonstrated both protective or harmful effects of nociceptor neurons on immune responses depending on the specific context of infection.

Until now, the role of the nociceptor neurons in bladder host defense has not been well defined. Here, we aim to uncover the crosstalk between nociceptor neurons and host immune response during UPEC infection. We hypothesized that UPEC could directly stimulate nociceptor neurons and affect the bladder immune microenvironment. In the present study, the inflammation, bladder urothelial barrier function and bacterial load were investigated after ablation nociceptor neurons. We determined whether nociceptor neurons limited the recruitment and function of neutrophils and macrophages. And we want to figure out the underlying mechanisms.

Materials and Methods

Mice and Nociceptor Neuron Ablation Model

Four-week-old female C57BL/6J mice were purchased from the Shandong University Experimental Animal Center. All mouse experiments were conducted according to protocols approved by Laboratory Animal Ethical and Welfare Committee of Shandong University Cheeloo College of Medicine (No. 20085) and in accordance with the guidelines of the Care and Use of Laboratory Animals (National Institutes of Health, Bethesda, MD, USA).

Four-week-old female C57BL/6J mice were anesthetized with isoflurane and injected intrathecally at L4-L5 with capsaicin (10 μ g, Meilunbio #MB6186) or vehicle (10% Tween 80, saline) for 2 days by a luer-tipped Hamilton syringe in a volume of 5 μ L with a 30-gauge needle. TRPV1⁺ nerve terminals were ablated after 24 hours by intrathecal capsaicin injection, and this effect could sustain for at least 8 weeks.^{18,19} Mice were bred in the animal facility of Shandong University until experiments.

Eight-week-old female C57BL/6J mice were anesthetized with isoflurane and injected intrathecally at L4-L5 with capsaicin (0.5 μ g, Meilunbio #MB6186) or vehicle (10% Tween 80, saline) for once by a luer-tipped Hamilton syringe with a 30-gauge needle.

Bacterial Strain, Culture and Mouse UTI Model

Uropathogenic wild-type *E. coli* strain CFT073 (American type culture collection, 700,928) was grown at 37 °C with 5% CO₂ in Luria-Bertani broth for 24 hours and resuspended in PBS to an optical density at 600 nm of 0.6. To induce cystitis, mice were anesthetized with isoflurane, then given 5×10^7 *E. coli* strain CFT073 in 60 μ L PBS by transurethral inoculation via a 0.28 mm catheter. CO₂ inhalation was used for euthanasia.

Bacterial Load Assessment

A total of 22–24 mouse urine in each group were collected at 24 hours post-infection and underwent serial dilution in PBS for 8 times. Ten microlitres of diluted sample was plated on Difco MacConkey agar plates. After incubation overnight at 37 °C, the number of urine colony-forming units (CFUs) was counted.

Ex vivo Gentamicin Protection Assays

A total of 12 mouse bladders in each group were collected at 24 hours post-infection and cultured in DMEM medium containing gentamicin (100 µg/mL) for 1 hour to kill extracellular bacteria. Add two sterile 3mm grinding beads to the bladder tissue and grind the tissue with a tissue grinder (Servicebio, China) for 90s at a frequency of 120 Hz, twice (representing invaded bacteria, the intracellular fraction). The next steps were the same as those of CFUs. The number of invaded bacteria was counted.

Western Blotting

Five mouse bladders of each group were homogenized with RIPA buffer (Beyotime Biotechnology, P0013B). Following 30 min reaction on ice, the tissue debris was pelleted by centrifugation (14,000g, 15 min, 4 °C). The supernatant was collected, and its concentration was determined by using bicinchoninic acid (BCA, Beyotime Biotechnology, P0010). Protein samples were heated for 10 min to 99 °C with loading buffer. Protein samples were separated to SDS-PAGE and were transferred to polyvinylidene difluoride membranes. The membranes were blocked with 5% skim milk for 1.5 hours at room temperature and incubated overnight at 4 °C with primary antibodies (TRPV1, 1:1,000, Abcam #ab203103). GAPDH (1:2,000, Abways #AB0037) was used as the referenced protein. After three washing times with Tris-buffered saline with tween-20 (TBST) for 10 min each, membranes were incubated with HRP-conjugated secondary antibodies (1:5,000, Cell Signaling Technology, #7076) for 1 hour at room temperature and washed three times with TBST. Signaling was detected with Amersham ImageQuant 800.

Histological Examination

Five to six mice of each group were sacrificed by CO₂ inhalation. Bladders were immersed in 4% paraformaldehyde, embedded in paraffin and sectioned. Bladder tissue slides were stained with hematoxylin and eosin (H&E). Stained slides were imaged by an Olympus microscope digital camera.

Immunofluorescence Analysis

Five L5-S1 DRG samples of each group and 4 bladders of each group were collected and sectioned. Paraffin sections were deparaffinized and heated to retrieve antigens. Next, the samples were removed endogenous peroxidase and blocked by 5% serum in 1% BSA for 1 hour at room temperature. The TRPV1 primary antibody (1:500, Abcam #ab203103) was incubated overnight at 4 °C with DRG tissue sections. The F4/80 antibody (1:400, Cell Signaling #30325) was incubated overnight at 4 °C with bladder tissue sections. The next day, the sections were placed at room temperature for 1 hour, followed by washing three times with phosphate buffered saline (PBS). Antigen-antibody complexes for DRG samples were detected with Alexa Fluor 594 goat anti-mouse IgG (1:200, Yeasen # 33212ES60) and antigen-antibody complexes for bladder samples were detected with Alexa Fluor 594 donkey anti-rabbit IgG (1:200, Yeasen # 34212ES60) at 37 °C for 1 hour. After DAPI staining to reveal the nuclei, the images were captured under fluorescence microscope (Olympus, Japan).

WGA

WGA staining was modified from previous research.⁹ Four bladder samples of each group were collected and sectioned. Bladder paraffin sections were processed as described above. After blocking, WGA-FITC (1:200, GeneTex #GTX01502) was incubated for 1 hour at room temperature with bladder tissue sections. After DAPI staining, the images were captured under a fluorescence microscope.

Trypan Blue

Trypan blue assay was modified from previous research.²⁰ At 24 hours post-infection, 4 mice of each group were anesthetized with isoflurane, then slowly given 1% trypan blue in PBS (60 µL) by transurethral delivery into bladder. Thirty minutes after trypan blue given, bladders were collected, washed with PBS and taken images.

Dorsal Root Ganglia Neuron Collection and Calcium Imaging

DRG from 8-week-old mice were dissected and transferred into neurobasal medium (Thermo Fisher), dissociated in collagenase type 4 (1 mg/mL, Biochem #LS004188) and dispase II (25 mg/mL, Solarbio #D6430) in HEPES-buffer saline (sigma) for 30 min

at 37 °C. After supernatant were removed, dissociated DRG were washed with DMEM (10% FBS) and centrifuged for 3 min at 500g at room temperature. Cells were resuspended in neurobasal medium (Thermo Fisher) and plated on 14 mm cell climbing dishes (Solarbio #YA0350) treated with poly-D-Lysine (2.5 mg/mL, Beyotime) in advance. For calcium imaging, cells were treated with 10 μM Fura-2 AM (Thermo Fisher) for 30 min in neurobasal medium at 37 °C and washed. Fura-2 AM was excited by alternating 340/380 nm and imaged by inverted microscope and camera (Nikon, Princeton Instruments). Images of 340/380 ratio were processed and analyzed by NIS-software (Nikon). Capsaicin (1 μM, Meilunbio #MB6186), live CFT073, LPS (10 ng/mL, sigma #L2630) were applied in calcium imaging.

Enzyme-linked immunosorbent assays (ELISA) 3 bladders of each group were collected at 0, 8, 24 hours post-infection and homogenized with PBS. Bladder tissue debris was transferred into a centrifuge tube and incubated with shaking (500rpm) for 15min at 4 °C. The supernatant from bladder tissue debris was collected after shake and quantified by a CGRP ELISAKit (Elabscience #M0215c) according to manufacturer's instructions.

PCR

Total RNA was extracted by using TRAzol (Invitrogen #15596018) according to the manufacturer's instructions. Extracted RNA was synthesized into cDNA using PrimeScript RT Master Mix (Accurate Biology). Synthesized cDNA was used for RT-PCR with SYBR Green Pro Taq Mix (Accurate Biology, AG11701) following the manufacturer's instructions. The result of mRNA relative expression levels was analyzed by the $2^{-\Delta\Delta C_t}$ method. GAPDH was used as the referenced gene. The following primers were used: mus-IL1β-F: 5'-AATGCCACCTTTTGACAGTGATG-3', mus-IL-1β-R: 5'-AGCTTCTCCACAGCCACAAT-3'; mus-IL6-F: 5'-ACAAAGCCAGAGTCCTTCAGA-3', mus-IL6-R: 5'-TGTGACTCCAGCTTATCTCTTG-3'; mus-IL10-F: 5'-GTAGAAGTGATGCCCCAGGC-3', mus-IL10-R: 5'-CACCTTGGTCTTGGAGCTTATT-3'; mus-Arg1-F: 5'-CTCC AAGCCAAAGTCCTTAGAG-3', mus-Arg1-R: 5'-AGGAGCTGTCATTAGGGACATC-3'; mus-Trpv1-F: 5'-TTCTCGTGGAGCCCTTGAAC-3', mus-Trpv1-R: 5'-CGATAGTAAGCAGCCGTGGT-3'. mus-GAPDH-F: 5'-GCCTCGTCCCGTAGACAAAAT-3'; mus-GAPDH-R: 5'-GTGACCAGGCGCCAATA-3'.

Flow Cytometry

Three to five bladder tissues of each group were dissociated in Liberase TL (0.5 mg/mL, Merck#05401020001) and dispase II (20 mg/mL, Merck#D4693) in HEPES-buffer saline (sigma) for 120 min at 37 °C. Dissociated tissues were filtered through 70 mm mesh and resuspended in HBSS buffer with 2% PFA. Cells were centrifuged at 500g for 3 min and resuspended in HBSS buffer. Immune cells were separated by 40% and 80% Percoll solution before flow cytometry. Surface antigens were stained and fixated and permeabilized, then stained intracellular proteins. Antibodies used for staining: anti-CD45.2-AF700 (1:200, Biolegend# 109822), anti-CD11b-APC-CY7 (1:200, Biolegend# 101226), anti-Ly-6G-FITC (1:200, Biolegend# 127606), anti-F4/80-PE (1:200, Biolegend# 157304), anti-CD86-FITC (1:200, Biolegend# 105110), anti-CD206-APC (1:200, Biolegend# 141708). We excluded dead cells by using a live cell stain (Aqua™ Fixable viability, Biolegend). It was centrifuged at 500g for 3 min and resuspended in HBSS buffer. Flow cytometry was conducted on Gallios flow cytometry (Beckman). Data were analyzed by FlowJo software.

Neutrophils and Macrophages Culture

Mice were euthanized by CO₂ inhalation and dissected femurs and tibias. Bone marrow was collected by PBS flushing. Cells were centrifuged at 1000rpm for 5 min. Then, supernatant was removed. Cells were resuspended in red blood cell lysis buffer (5 mL, Beyotime #C3702) for 5 min at room temperature. Added PBS (5mL) and centrifuged at 1000rpm for 5 min. Cells were resuspended and cultured in low glucose DMEM (sigma #D6046) with macrophage colony stimulating factor (MCSF) (25 ng/mL, Abcam #ab129146) and 10% FBS. After 3 days of cell culture, the fresh culture medium was replaced, and then cultured for 4 days, bone marrow-derived macrophage (BMDM) could be used for subsequent experiments.

For neutrophil culture, peripheral blood of mice was collected and centrifuged at 500g for 5 min to separate serum. Added the same volume of 0.9% NaCl solution and mixed. Ficoll neutrophil isolation solution (TBD #LST1077-1) was used according to the manufacturer's instructions. Next, layer of red blood cell and neutrophil was collected. Cells were centrifuged at 1200rpm for 5 min and resuspended in red blood cell lysis buffer (Beyotime #C3702) for 5 min at room

temperature (the process was repeated three times). Then, cells were cultured in 1640 medium (sigma #R8758) with 10% FBS and serum.

Neutrophil Bactericidal Activity

Neutrophils were treated with CGRP (1 μ M, GenScript #RP11095) or vehicle for 2 hours in advance. Neutrophils (10^7 cells per well) were incubated with CFT073 (10^7 CFU) in 1640 medium with 10% FBS and mouse serum for 1 hour at 37 °C. The control group did not add neutrophils but added the same number of CFT073. After 1 hour, cells were centrifuged at 1000rpm for 5 min. Then, the supernatant was centrifuged at 5000rpm for 5 min to collect extracellular bacteria. Centrifuged cells were resuspended in 1640 medium with 10% FBS and gentamicin (100 μ g/mL) for 1 hour to kill adherent extracellular bacteria. Used 0.5% Triton-100 (Beyotime #ST797) to lyse cells and collected intracellular bacteria. Bacteria was undergoing serial dilution in PBS and incubated overnight at 37 °C. The number of neutrophil bactericidal = the control group's CFUs-extracellular CFUs-intracellular CFUs. The number of neutrophil phagocytosis = the control group's CFUs-extracellular CFUs.

MPO Assay

Neutrophils (10^6 cells/well) were treated with CGRP (1 μ M, GenScript #RP11095) or vehicle and incubated with CFT073 (10^5 CFU) immediately in 1640 medium with 10% FBS for 1 hour. Collected supernatant for myeloperoxidase (MPO) activity analysis by a MPO test kit (Elabsience #K074-S) according to manufacturer's instructions.

pH Probe

BMDMs were plated on 14 mm cell climbing dishes (Solarbio #YA0350) in advance and treated with CGRP or vehicle for 24 hours. The pH levels of mouse BMDM were measured by a pH probe (LysoTracker Deep Red, Invitrogen, L12492). BMDMs were treated with pH probe for 30 min at 37 °C in 5% CO₂. After DAPI staining, the images were captured under a fluorescence microscope.

RNA-Sequencing Experiment Analysis Method

Quality control: Raw data (raw reads) of fastq format were processed with fastp, an ultra-fast FASTQ preprocessor with useful quality. Clean data (clean reads) were obtained after quality control, adapter trimming, quality filtering and per-read quality cutting. All the downstream analyses were based on the clean data with high quality.

Read mapping to the reference genome: Reference genome and gene model annotation files were downloaded from genome website directly. Paired-end clean reads were aligned to the reference genome using HISAT2 v2.1.0 (hierarchical indexing for spliced alignment of transcripts), which is a highly efficient system for aligning reads from RNA sequencing experiments. HISAT2 uses an indexing scheme based on the Burrows-Wheeler transform and the Ferragina-Manzini (FM) index, employing two types of indexes for alignment: a whole-genome FM index to anchor each alignment and numerous local FM indexes for very rapid extensions of these alignments. HISAT2 is the fastest system currently available, with equal or better accuracy than any other method. HISAT2 was run with the default parameters.

Quantification of gene expression level: Featurecount was used to count the reads numbers mapped to each gene. The FPKM of each gene was calculated based on the length of the gene and reads count mapped to this gene. FPKM, expected number of fragments per Kilobase of transcript sequence per millions base pairs sequenced, considers the effect of sequencing depth and gene length for the reads count at the same time, and is currently the most commonly used method for estimating gene expression levels.

Differential expression analysis (for DESeq2 with biological replicates): Differential expression analysis of two conditions/groups (two biological replicates per condition) was performed using the DESeq R package (1.18.1). DESeq provides statistical.

Raw sequence read files are available in the NCBI Sequence Read Archive (SRA) under BioProject PRJNA783048.

Gene Set Variation Analysis

Gene set variation analysis (GSVA) R package was used to estimate the signaling pathways based on transcriptome sequencing data of each sample.²¹ We used Hallmark gene sets and KEGG gene sets as the reference to identify the most relevant pathways of BMDM with CFT073 infection in CGRP-treated samples compared with vehicle-treated samples.

BoNT/A and BIBN4096 Treatment

BoNT/A (0.2 U, Lanzhou biology) was systemically administered by intraperitoneal injection 24 hours before infection with CFT073, and BIBN4096 treatment (Tocris #4561) was systemically administered by intraperitoneal injection 2 hours before infection.

Statistical Analysis

Data were analyzed by GraphPad Prism software. A two-tailed unpaired Student's *t*-test was used for comparison between the two groups. $P < 0.05$ was considered to be significant.

Result

CFT073 Directly Stimulates Nociceptor Neurons That Release CGRP into Infected Bladder

Calcium imaging technique was used to observe the activation of DRG neurons in vitro. A few minutes after exposure, a strong calcium influx in DRG neurons was evoked by live CFT073 strain in vitro (Figure 1A). These DRG neurons that response to CFT073 can be further activated by capsaicin. We next determined whether LPS, a pathogenic factor of *E. coli*, could also induce calcium influx in DRG neurons. Similar to what other studies have reported,²² LPS could sensitize DRG neurons (Figure 1A).

We used high doses of capsaicin to ablate nociceptor neurons according to the previous studies^{18,19} (Figure 1B). It was found that high dose of capsaicin (Cap^h group) led to loss of TRPV1 neurons (Figure 1C) and decreased TRPV1 mRNA and proteins in the muscular layer of bladder (Appendix Figure 1A and B). It was also found in vivo that CFT073 invasion induced CGRP release at the infected bladder. A significant increase of CGRP levels was observed at 8 hours and 24 hours after CFT073 infected. Decreased CGRP was found in the bladder of Cap^h mice compared to the control group after UPEC infection (Figure 1D). It indicated that the release of CGRP was associated with TRPV1 neuron activation.

Nociceptor Neuron Activation Increases Bacterial Load and Aggravates UPEC-Induced Bladder Epithelial Barrier Dysfunction

Histopathologic analysis of bladder showed less tissue edema and inflammation in Cap^h mice compared to the control mice in response to UPEC infection (Figure 2A). To evaluate the function of the bladder barrier, we assessed the integrity of superficial epithelium by used wheat germ agglutinin-fluorescein isothiocyanate (WGA-FITC) as a probe.⁹ Twenty-four hours post-infection, WGA layer did not form complete structure and was even absent. This phenomenon was significantly alleviated in Cap^h group (Figure 2B). Epithelial integrity can also be assessed by examining barrier function following administration of trypan blue dye, which only penetrates damaged bladder epithelium. We observed strong trypan blue coloration in infected mice bladders and limited coloration of trypan blue into the bladder epithelium in Cap^h mice (Figure 2C). Twenty-four hours after UPEC infection, the number of urine colony-forming units (CFUs) and invaded bacteria were recorded. The results showed that Cap^h mice significantly reduced the number of CFUs and invaded bacteria relative to the vehicle group (Figure 2D and E). To investigate the activating effect of nociceptor fibers, we treated mice with low doses of capsaicin (Cap^L mice) at 2 hours before-infection. We found that the number of invaded bacteria was increased in Cap^L mice compared to the vehicles (Appendix Figure 1C). However, there was no statistical difference in CFUs between Cap^L and vehicle mice (Appendix Figure 1D).

CGRP Released by Nociceptors Suppresses Neutrophil Recruitment and Bactericidal Activity

A strong innate immune response is a sign of UTIs and necessary to eliminate infection. Neutrophils play a major bactericidal role during the innate immune response to UTIs.^{23,24} Flow cytometry analysis showed that more CD11b⁺Ly6G⁺ neutrophils were recruited in the bladder of Cap^h mice compared to vehicle group after UPEC infection (Figure 3A). Myeloperoxidase (MPO) is a peroxidase, abundantly expressed in neutrophils and plays an antibacterial function.²⁵ After CFT073 infection, neutrophils produced a large amount of MPO and this effect was inhibited by CGRP

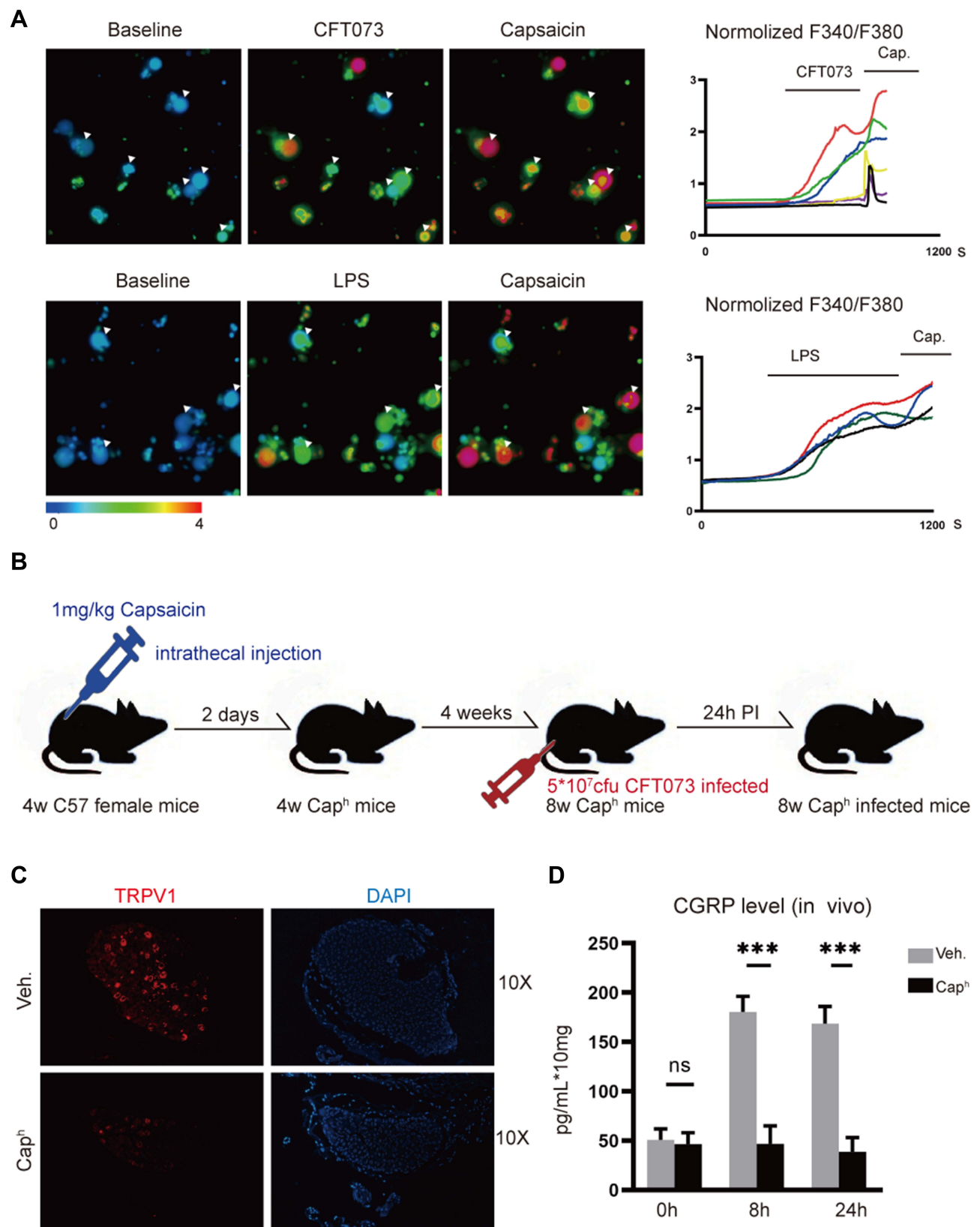


Figure 1 CFT073 induces neuron activation and CGRP release (A) Representative Fura-2 ratiometric fields (left) and calcium traces (right) of DRG neurons responding to CFT073 (5×10^7 CFUs), LPS (10 ng/mL) and capsaicin (1 μ M) ($n=3$). (B) Experimental schematic of TRPV1⁺ neuron ablation and CFT073-induced UTIs to mice. (C) Representative images of TRPV1⁺ (red) neurons by immunofluorescence assays ($n=5$). (D) Measurement of CGRP release with an ELISA kit. CGRP released from bladder (0, 8 and 24 hours) after CFT073 infection (5×10^7 CFUs) of vehicle-treated or Cap^h mice ($n=3$; ns, $P > 0.05$; *** $P < 0.001$).

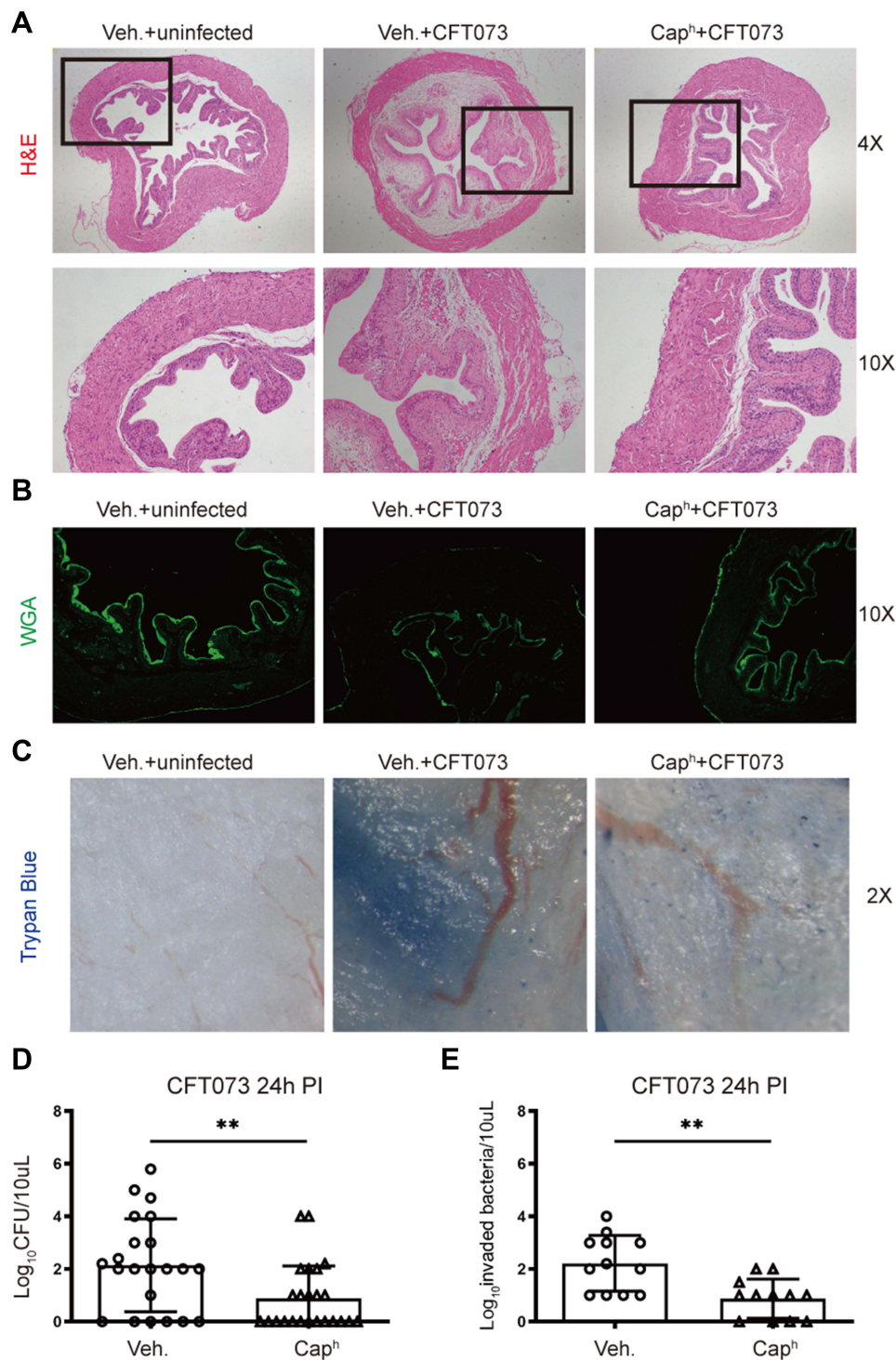


Figure 2 Nociceptor neurons mediate bladder epithelial function and bacterial load during UPEC infection. Vehicle-treated mice were randomly divided into uninfected or infected group. Cap^h mice were infected equivalent CFT073 (5×10^7 CFUs). **(A)** H&E Staining of bladders from groups “vehicle-uninfected”, “vehicle-infected” and “Cap^h-infected” (n=6). **(B)** Representative images of WGA-FITC in superficial bladder epithelial cells (n=4). **(C)** Representative images of trypan blue staining in bladders (n=4). **(D)** Bacterial load recovery (\log_{10} CFU) from urine in “Cap^h-infected” or “vehicle-infected” group (n =22-24; **P < 0.01). **(E)** Ex vivo gentamicin protection assays representing invaded bacteria in “Cap^h-infected” or “vehicle-infected” group (n =12; **P < 0.01).

(Figure 3B). The phagocytic function of neutrophils to CFT073 decreased slightly in CGRP-treated group compared with vehicle-treated group, which was not statistically significant (Figure 3C). We also found that CGRP inhibited mouse neutrophil killing of *E. coli* (Figure 3D).

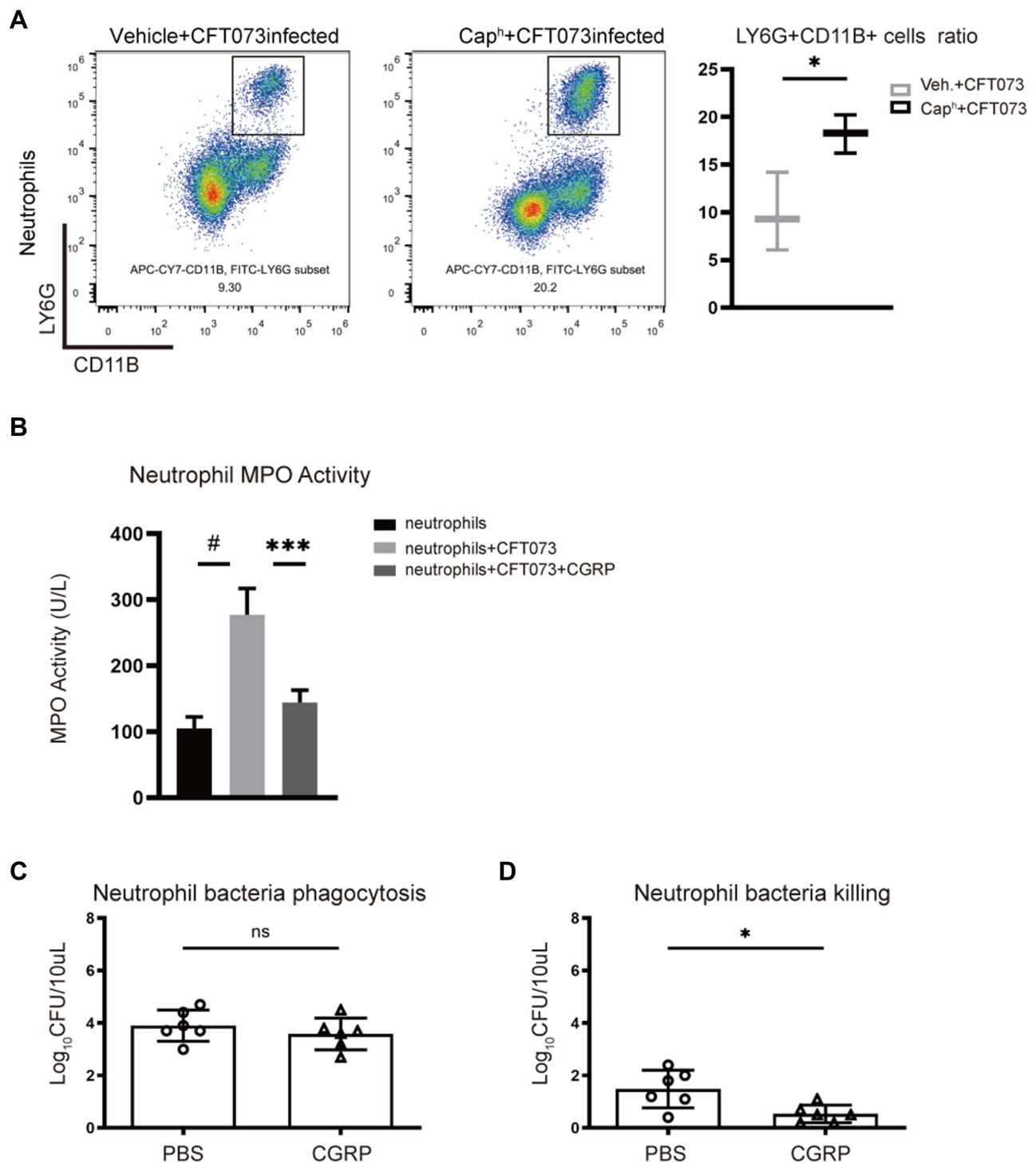


Figure 3 Nociceptor neurons suppress recruitment and bactericidal function of neutrophils (A) Representative FACS plots (left) showing neutrophils (CD11b+Ly6G+ gates) in Cap^h or vehicle-treated mouse bladders. Assessment ratio (right) of Cap^h or vehicle-treated mouse bladder neutrophils by flow cytometry analysis (n=3; *P < 0.05). Mouse neutrophils were co-cultured with CFT073 in presence of vehicle or CGRP (1μM) for 1 hour (B–D). (B) Myeloperoxidase (MPO) activity of neutrophils (n=5; ***P < 0.001; #P < 0.0001). (C) Bacterial phagocytosis of neutrophils (n=6; ns, P > 0.05). (D) Bacterial killing function of neutrophils (n=6; *P < 0.05).

CGRP Released by Nociceptor Neurons Causes Macrophage Proinflammatory Phenotype Polarization

Macrophage plays an important role in the defense of infection and the maintenance of bladder homeostasis.²⁶ Through analyzing Flow cytometry of UPEC-infected bladders, no difference of CD11b⁺F4/80⁺ macrophage recruitment was

observed in Cap^h mice compared with vehicle-treated mice (Figure 4A). Next, the localization of macrophages in the UPEC-infected bladder was evaluated. Immunofluorescence staining showed that F4/80-positive cells located close to bladder epithelium in Cap^h mice decreased slightly compared with vehicle-treated mice after UPEC infection (Figure 4B).

We next tested the polarization of macrophages through analyzing flow cytometry of UPEC-infected bladder. Less CD86⁺ M1 macrophages and more CD206⁺ M2 macrophages were found in Cap^h mice bladders compared to

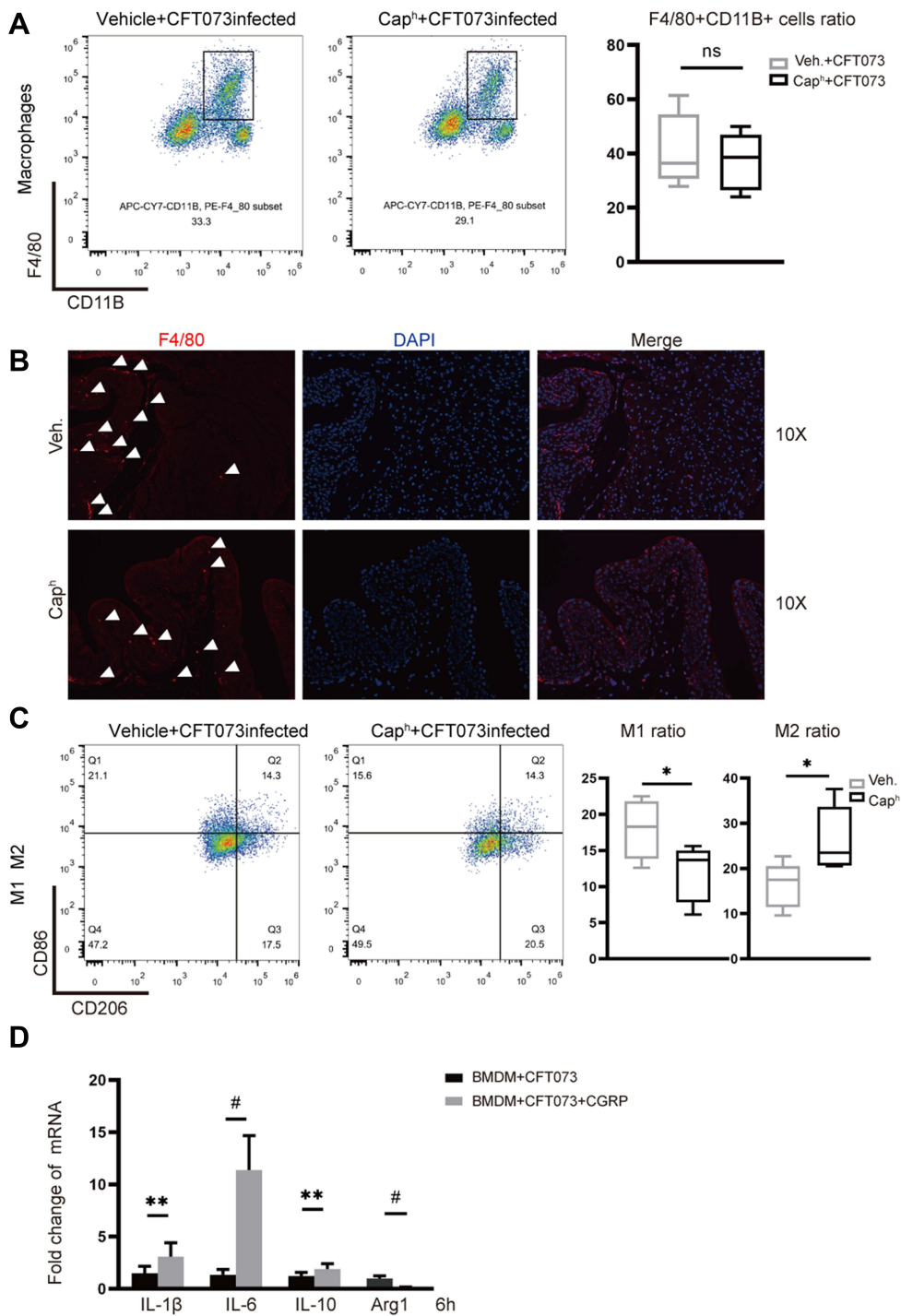


Figure 4 Continued.

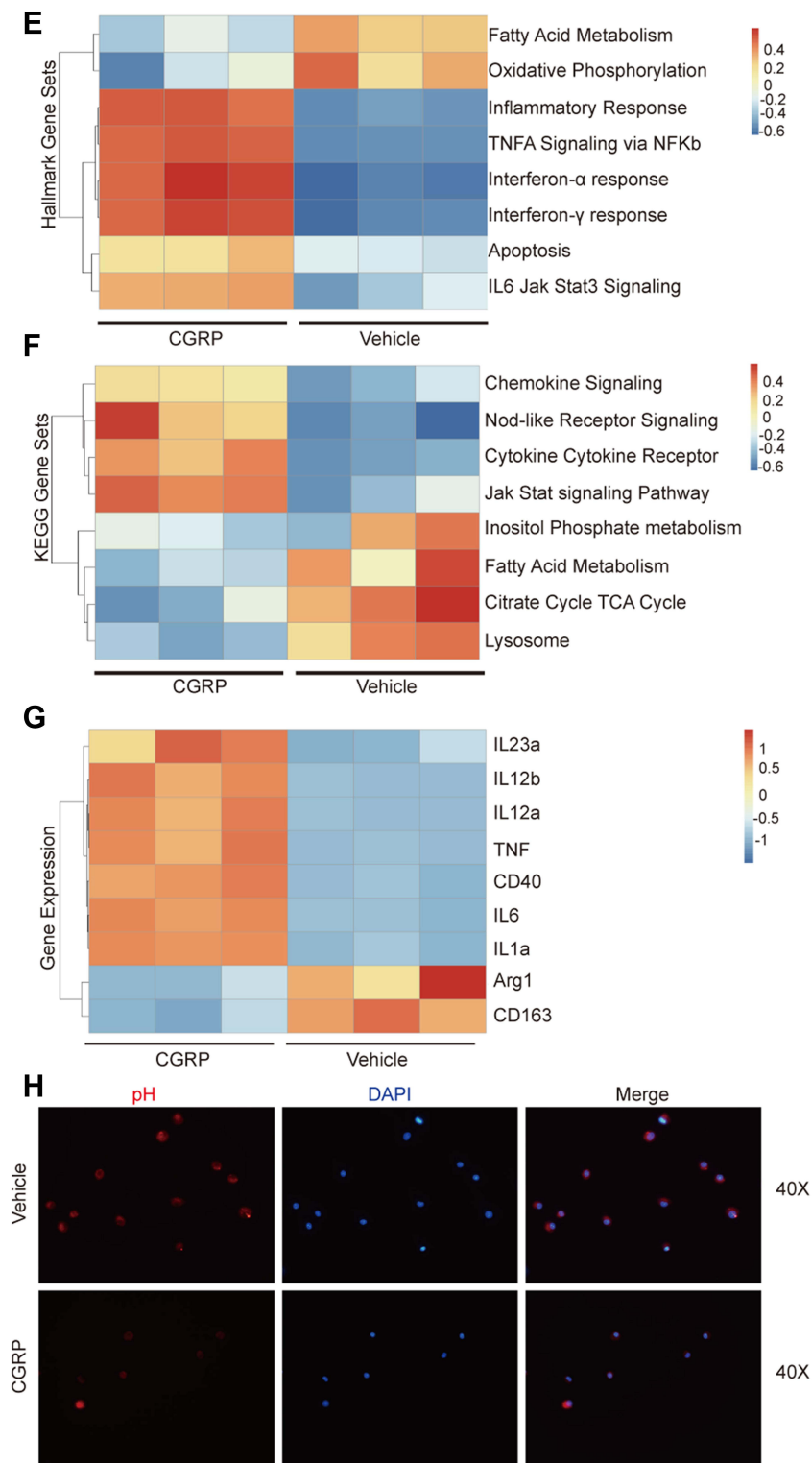


Figure 4 Nociceptor neurons affect polarization of macrophages (A) Representative FACS plots (left) showing macrophages (F4/80+ CD11B+) in Cap^h or vehicle-treated mouse bladders. Assessment ratio (right) of Cap^h or vehicle-treated mice bladder macrophages by flow cytometry analysis (n=5; ns, P > 0.05). (B) Representative images of the locations of F4/80-positive cell in Cap^h or vehicle-treated mice bladders by immunofluorescence assays (n=4). (C) Representative FACS plots (left) showing M1 (F4/80+CD11B+CD86+ gates) and M2 (F4/80+CD11B+CD206+) in Cap^h or vehicle-treated mouse bladders. Assessment ratio (right) of Cap^h or vehicle-treated mice bladder M1 and M2 by flow cytometry analysis (n=5; *P < 0.05). mRNA expression from mouse BMDM after 6 hours post-infection with CGRP or PBS-treated (D–G). (D) Measurement of mRNA of mouse macrophages polarization marker by PCR (n=3; **P < 0.01; [#]P < 0.0001). (E) Transcriptome analysis by Hallmark gene sets. (F) Transcriptome analysis by KEGG gene sets. (G) Differentially expressed genes for transcriptome analysis. (H) Representative images of pH probe (red) for the pH levels of mouse BMDM by immunofluorescence assays (n=6).

vehicle group (Figure 4C). We hypothesized that the release of CGRP from nociceptor neurons resulted in mouse macrophage polarization in the UPEC-infected bladder, which may lead to the destruction of bladder epithelium homeostasis and the aggravation of inflammation. In vitro, experiment using mouse bone marrow-derived macrophages (BMDMs) showed that CGRP could increase the expression of M1 proinflammatory genes (IL-1b, IL-6) and decrease the expression of M2 anti-inflammatory gene (Arg-1) (Figure 4D).

Transcriptome analysis by Hallmark gene sets (Figure 4E) showed that majority of differential genes in BMDM treated by CGRP were belonging to “inflammatory response” pathway, including “TNF α signaling via NF-kappa B” pathway, “interferon α response” pathway and “interferon β response” pathway. It suggested a high level of inflammation state in the presence of CGRP. Transcriptome analysis also showed that “oxidative phosphorylation” pathway and “fatty acid metabolism” pathway were more active in vehicle-treated BMDM. Previous study reported that M2 macrophages had enhanced TCA cycle activity, mitochondrial oxidative phosphorylation activity and fatty acid utilization compared to M1 macrophages.²⁷ Meanwhile, we analyzed RNA-seq data by KEGG gene sets (Figure 4F) and found that genes with increased expression in BMDM treated by CGRP were belonging to “cytokine–cytokine receptor interaction” pathway and “chemokine signaling” pathway. Meanwhile, genes with increased expression in BMDM treated by vehicle were belonging to “citrate TCA cycle” pathway and “lysosome” pathway. This result was also consistent with the result of Hallmark gene sets. The detailed gene expression of M1 and M2 macrophages showed that more TNF, IL-6, IL-1a, CD40, IL-12a, IL-12, IL-23a and less Arg1, CD163 were expressed in CGRP treatment group compared to vehicle treatment group (Figure 4G).

Lysosome plays an important role in the interaction between macrophages and bacteria, which is an acidic organelle, and low pH value is the key to its normal function.²⁸ Using a fluorescent pH probe, we observed that in the presence of CGRP, the intracellular pH of macrophages increased (Figure 4H). This finding was also related with the RNA-seq data analyzed by KEGG database (Figure 4F).

BoNT/A Injection and CGRP Receptor Antagonism Applied in CFT073 Infection

We next investigated the effect of the BoNT/A treatment (inhibition of neural vesicle release) and CGRP receptor antagonism (BIBN4096) on the host response of bladder. Systemic BoNT/A treatment, when administrated 24 hours before infection, or systemic BIBN4096 treatment, when administrated 2 hours before infection, were associated with reduced bladder cystitis (Figure 5A), more complete WGA layer (Figure 5B), less epithelium damage (Figure 5C) and increased bacterial clearance (Figure 5D), compared to mice treated with vehicle alone.

BoNT/A or BIBN4096 treatments increased the recruitment of neutrophils to the infected bladder compared to untreated mice (Figure 5E). The result also showed less CD86⁺ M1 macrophages in bladder after BoNT/A or BIBN4096 injections compared to vehicles. CD206⁺ M2 macrophages were slightly increased in BIBN4096 treatment group (Figure 5F).

Taken together, our findings suggested that nociceptor neurons inhibited the recruitment and function of neutrophils and macrophages during UPEC infection (Figure 6).

Discussion

A fundamental role of nociceptor sensory neurons is to protect organisms from danger by detecting stimuli and eliciting pain. In this study, we treated mice with high dose of capsaicin by intrathecal injection to ablate nociceptors and identified a crucial role of sensory neurons in host response to UPEC invasion. UPEC and its pathogenic factor LPS could directly activate nociceptor neurons, which inhibited the recruitment of neutrophils, the polarization of macrophages and the killing of UPEC. These inhibitive mechanisms were linked to neuronal release of CGRP, which regulated neutrophils and macrophage functions both in vivo and in vitro. Notably, it has been found by recent studies that neuropeptides can have a direct regulatory effect on innate immune cells.²⁹ In the gut muscularis layer, when activated by bacterial infection, norepinephrine released from extrinsic sympathetic innervation mediated alternative activation of muscularis macrophages and induced fast tissue protection.³⁰ Neuropeptide neuromedin U activates ILC2 and causes type 2 inflammation to promote worm expulsion in enteric mucosal sites.³¹ The present study indicated an important role

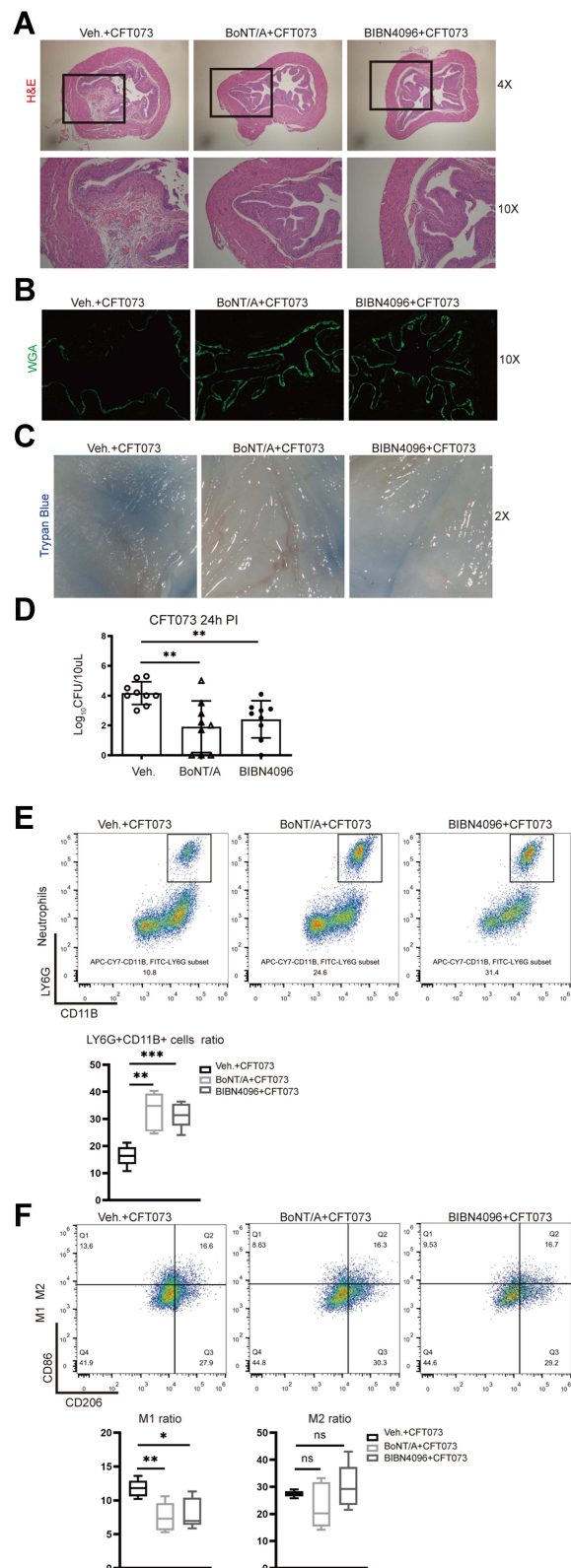


Figure 5 BoNT/A and BIBN4096 treatment block neural signal (A–C) Representative images show bladder inflammation and uroepithelium damage for groups “vehicle-infected”, “BoNT/A-infected” and “BIBN4096-infected”. (A) H&E staining (B) WGA-FITC and (C) trypan blue staining (n=3–5). (D) Bacterial load recovery (log₁₀ CFU) from urine for each group (n =9/group; **P < 0.01). (E) Representative FACS plots (left) showing neutrophils (CD11b+Ly6G+ gates) in Cap^h or vehicle-treated mouse bladders. Assessment ratio (right) of Cap^h or vehicle-treated mice bladder neutrophils by flow cytometry analysis (n=5; **P < 0.01; ***P < 0.001). (F) Representative FACS plots (left) showing M1 (F4/80+CD11B+CD86+ gates) and M2 (F4/80+CD11B+CD206+) in Cap^h or vehicle-treated mouse bladders. Assessment ratio (right) of Cap^h or vehicle-treated mice bladder M1 and M2 by flow cytometry analysis (n=5; ns, P > 0.05; *P < 0.05; **P < 0.01).

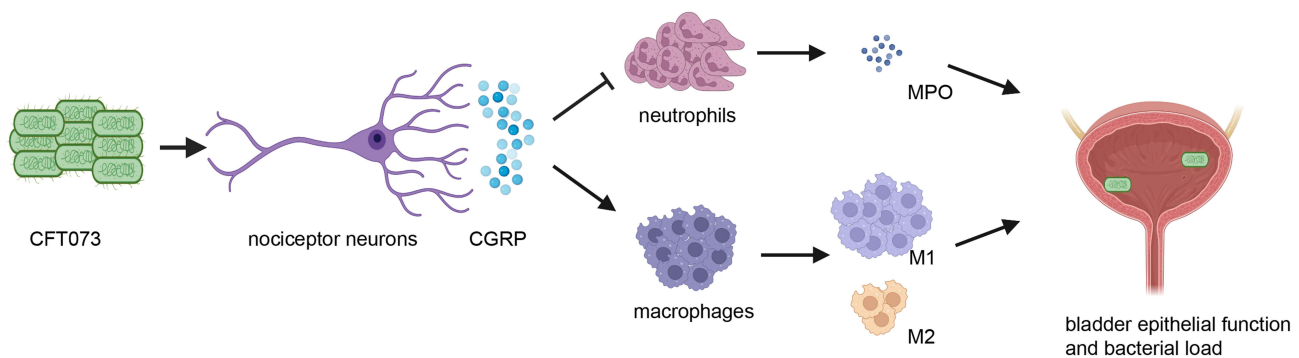


Figure 6 A schematic diagram of the results. UPEC could directly stimulate nociceptor neurons, releasing CGRP into the infected bladder which inhibited the recruitment of neutrophils, MPO releasing and affected the polarization of macrophages, and finally caused bladder inflammation, epithelial barrier dysfunction and increased bacterial load.

of CGRP in the host response to UTIs. Previous studies have shown that CGRP acts variously, including on vascular endothelial cell to mediate vasodilation³² and on epithelial cells to regulate inflammation.³³ In addition, CGRP receptor is highly expressed in neutrophils, monocytes and macrophages.¹⁵ According to the results of the present study, blocking neuro-immune suppressive effect through CGRP may be a potential strategy to treat UTIs.

The present study found that UPEC and LPS could directly stimulate nociceptor neurons. LPS is the most important ligand for Toll-Like Receptor 4 (TLR4) and promotes the intracellular progression of UPEC in urinary tract.³⁴ Toll-like receptors (TLRs) are key molecules in the immune system.³⁵ The other study found that LPS could sensitize trigeminal sensory neurons via TLR4.²² It would be interesting to know if the LPS stimulates nociceptor neurons through TLR4 or if some other structures of UPEC cloud are exacerbating the immune response through nociceptor neurons.

The present study found that nociceptor neuron activation influenced the polarization of macrophages. Specifically, the neuropeptide CGRP promoted the polarization of M1 in the context of UPEC infection. In the presence of CGRP, UPEC-induced macrophages also expressed more pro-inflammation factors and fewer anti-inflammatory factors. Abundant macrophages are located in the urinary tract submucosa.⁴ Macrophages have bactericidal activity, but this activity seems to be less critical for killing bacteria than that for neutrophils.^{23,24} However, macrophages do play an important role in inflammation resolution after bacteria are cleared.^{36,37} Traditionally, macrophage polarization has been broadly divided into two groups: M1 and M2 macrophages. Whereas M1 macrophages are highly inflammatory by producing inflammatory mediators, M2 macrophages are less inflammatory and participate in tissue repair. Meanwhile, it is widely believed that M1 macrophages are microbicidal and M2 macrophages are poorly microbicidal.³⁸ Inflammation can be a double-edge sword for infections. Uncontrolled or prolonged M1 polarization can be deleterious for the host causing tissue damage and further bacterial development.³⁹ In patients with severe sepsis, a substantial existence of M1-phenotype cytokines was positively correlated with high mortality.⁴⁰ In our study, the release of CGRP during UPEC infection induced excessive M1 polarization, which led to tissue injury and disposed the bladder to further infections. M1 polarization induced by CGRP was supposed to play a negative role in the host defense of UPEC.

The present study also found that nociceptor neuron activation suppressed neutrophil recruitment and function in the progression of UPEC infection. Neutrophils are the most potent bactericidal phagocytes and represent the most population of circulating leukocytes in the blood.²⁷ In UTIs, neutrophils are the first immune cells to be recruited to the infected bladder. A rapid and strong neutrophilia is a feature of innate immune activation. The number of neutrophils is closely related to the bacterial burden in UTIs. With the increase of the bacterial number, neutrophils also increase accordingly.^{4,23} Neutrophil activation is a mechanism of the body defense to infection. However, excessive and dramatic neutrophilia is also harmful to surrounding bladder tissues due to reactive oxidants and other toxic substance releasing. Thus, we consider that neural suppression of neutrophils during bacterial invasion may be a feedback mechanism for host self-protection to limit injury from excessive M1 inflammation.

The crosstalk between neutrophils and macrophages might be involved in the neuro-immuno-modulation of host response to UPEC infection. Previous studies demonstrated that an alternatively activated neutrophil can interact with macrophages to upregulate M2 markers during helminth infection.⁴¹ It is assumed that the interaction existed between macrophages and neutrophils during infections.^{38,42} It is also well known that macrophages recruit neutrophils in the early stage of infection and injury^{7,43} and macrophages phagocytize neutrophils in the late stage of infection to prevent further injury.⁴⁴ The present study found that nociceptor neuron activation led to decreased neutrophil recruitment and increased M1 polarization and decreased expression of M2 markers. There are two possibilities accounting for this result. Firstly, the inhibitory effect of nociceptor nerve on neutrophils might be greater than the effect of M1 macrophages on neutrophil recruitment. Secondly, macrophages might begin to phagocytize and clear neutrophils at this stage of infection.

BoNT/A has been shown to reduce pain by suppressing neuropeptides released from nociceptor sensory neurons.⁴⁵ BoNT/A has been widely used in cosmetic dermatology, migraine and interstitial cystitis/bladder painful syndrome.^{46–48} In the present study, BoNT/A was used to inhibit the release of CGRP. In addition, BoNT/A also impacts the release of ATP, acetylcholine, substance P and other neuropeptides.⁴⁹ CGRP receptor antagonist BIBN4096 was used to further confirm that the effect of the immune response was mediated by CGRP. The results demonstrated that both BoNT/A and BIBN4096 can block neuronal suppression of the immune response during CFT073 infection.

Conclusion

This study revealed that nociceptor neurons are closely involved in the host response to UPEC infection. CGRP might be a potential therapeutic target for the prevention and treatment of UTIs. Future studies are needed to dissect the exact roles played by nociceptor neurons in this process. Exploring how neurons modulate immune responses may break fresh ground for the treatment of UTIs.

Abbreviations

UTIs, Urinary tract infections; CGRP, Calcitonin gene-related peptide; LPS, Lipopolysaccharide; BoNT/A, Botulinum neurotoxin A; UPEC, Uropathogenic *Escherichia coli*; DRG, Dorsal root ganglia; WGA, Wheat germ agglutinin fluorescein isothiocyanate; CFUs, Colony-forming units; MPO, Myeloperoxidase; BMDMs, Bone marrow-derived macrophages; MCSF, Macrophage colony stimulating factor; BCA, Bicinchoninic acid; TNF, Tumor necrosis factor; IL, Interleukin; GAPDH, Glyceraldehyde-3-phosphate dehydrogenase; H&E, Hematoxylin & eosin; KEGG, Kyoto Encyclopedia of Genes and Genomes; GSEA, Gene set variation analysis; PBS, Phosphate-buffered saline; TRPV1, Transient receptor potential V1; DMEM, Dulbecco's modified Eagle's medium; FBS, Fetal bovine serum; PFA, Paraformaldehyde; HBSS, Hank's balanced salt solution; DAPI, 4',6-diamidino-2-phenylindole; PBS, Phosphate buffered saline; SDS-PAGE, Sodium dodecyl sulfate polyacrylamide gel electrophoresis; TBST, Tris-buffered saline with tween-20; HPF, High power field.

Acknowledgments

Thank Professor Xiulin Zhang for her technical help in the experiment.

Funding

This study was supported by the Funds of the National Natural Science Foundation of China (Grant No. 81970661; 81900637), the Tai Shan Scholar Foundation to Benkang Shi (ts201511092) and Shandong Medical and Health Science and Technology Development Plan Project (2018WS333).

Disclosure

The authors declare that they have no conflict of interest.

References

1. Öztürk R, Murt A. Epidemiology of urological infections: a global burden. *World J Urol.* 2020;38(11):2669–2679. doi:10.1007/s00345-019-03071-4
2. Flores-Mireles AL, Walker JN, Caparon M, Hultgren SJ. Urinary tract infections: epidemiology, mechanisms of infection and treatment options. *Nat Rev Microbiol.* 2015;13(5):269–284. doi:10.1038/nrmicro3432
3. Behzadi P, Urbán E, Matuz M, Benkő R, Gajdács M. The role of gram-negative bacteria in urinary tract infections: current concepts and therapeutic options. *Adv Exp Med Biol.* 2021;1323:35–69. doi:10.1007/5584_2020_566
4. Abraham SN, Miao Y. The nature of immune responses to urinary tract infections. *Nat Rev Immunol.* 2015;15(10):655–663. doi:10.1038/nri3887
5. Wu J, Miao Y, Abraham SN. The multiple antibacterial activities of the bladder epithelium. *Ann Transl Med.* 2017;5(2):35. doi:10.21037/atm.2016.12.71
6. Haraoka M, Hang L, Frendeus B, et al. Neutrophil recruitment and resistance to urinary tract infection. *J Infect Dis.* 1999;180(4):1220–1229. doi:10.1086/315006
7. Schiwon M, Weisheit C, Franken L, et al. Crosstalk between sentinel and helper macrophages permits neutrophil migration into infected uroepithelium. *Cell.* 2014;156(3):456–468. doi:10.1016/j.cell.2014.01.006
8. Mulvey MA, Lopez-Boado YS, Wilson CL, et al. Induction and evasion of host defenses by type 1-Piliated uropathogenic *Escherichia coli*. *Science.* 1998;282:1494–1497. doi:10.1126/science.282.5393.1494
9. Choi HW, Bowen SE, Miao Y, et al. Loss of bladder epithelium induced by cytolytic mast cell granules. *Immunity.* 2016;45(6):1258–1269. doi:10.1016/j.immuni.2016.11.003
10. Hozzari A, Behzadi P, Kerishchi KP, Sholeh M, Sabokroo N. Clinical cases, drug resistance, and virulence genes profiling in Uropathogenic *Escherichia coli*. *J Appl Genet.* 2020;61(2):265–273. doi:10.1007/s13353-020-00542-y
11. Leng WW, Chancellor MB. How sacral nerve stimulation neuromodulation works. *Urol Clin N Am.* 2005;32(1):11–18. doi:10.1016/j.ucl.2004.09.004
12. Basbaum AI, Bautista DM, Scherrer G, Julius D. Cellular and molecular mechanisms of pain. *Cell.* 2009;139(2):267–284. doi:10.1016/j.cell.2009.09.028
13. Pinho-Ribeiro FA, Verri WA, Chiu IM. Nociceptor sensory neuron-immune interactions in pain and inflammation. *Trends Immunol.* 2017;38(1):5–19. doi:10.1016/j.it.2016.10.001
14. Pinho-Ribeiro FA, Baddal B, Haarsma R, et al. Blocking neuronal signaling to immune cells treats streptococcal invasive infection. *Cell.* 2018;173(5):1083–1097. doi:10.1016/j.cell.2018.04.006
15. Chiu IM, Heesters BA, Ghasemlou N, et al. Bacteria activate sensory neurons that modulate pain and inflammation. *Nature.* 2013;501(7465):52–57. doi:10.1038/nature12479
16. Baral P, Umans BD, Li L, et al. Nociceptor sensory neurons suppress neutrophil and $\gamma\delta$ T cell responses in bacterial lung infections and lethal pneumonia. *Nat Med.* 2018;24(4):417–426. doi:10.1038/nm.4501
17. Kashem SW, Riedl MS, Yao C, et al. Nociceptive sensory fibers drive interleukin-23 production from CD301b+ dermal dendritic cells and drive protective cutaneous immunity. *Immunity.* 2015;43(3):515–526. doi:10.1016/j.immuni.2015.08.016
18. Cavanaugh DJ, Lee H, Lo L, et al. Distinct subsets of unmyelinated primary sensory fibers mediate behavioral responses to noxious thermal and mechanical stimuli. *P Natl Acad Sci USA.* 2009;106(22):9075–9080. doi:10.1073/pnas.0901507106
19. Shields SD, Cavanaugh DJ, Lee H, Anderson DJ, Basbaum AI. Pain behavior in the formalin test persists after ablation of the great majority of C-fiber nociceptors. *Pain.* 2010;151(2):422–429. doi:10.1016/j.pain.2010.08.001
20. Levin RM, Wein AJ, Whitmore K, et al. Trypan blue as an indicator of urothelial integrity. *Neurourol Urodyn.* 1990;9(3):269–279. doi:10.1002/nau.1930090305
21. Hanzelmann S, Castelo R, Guinney J. GSEA: gene set variation analysis for microarray and RNA-seq data. *BMC Bioinform.* 2013;14(1):7. doi:10.1186/1471-2105-14-7
22. Diogenes A, Ferraz CCR, Akopian AN, Henry MA, Hargreaves KM. LPS sensitizes TRPV1 via activation of TLR4 in trigeminal sensory neurons. *J Dent Res.* 2011;90(6):759–764. doi:10.1177/0022034511400225
23. Dale DC, Boxer L, Liles WC. The phagocytes: neutrophils and monocytes. *Blood.* 2008;112(4):935–945. doi:10.1182/blood-2007-12-077917
24. Kantari C, Pederzoli-Ribeil M, Witko-Sarsat V. The role of neutrophils and monocytes in innate immunity. *Contrib Microbiol.* 2008;15:118–146. doi:10.1159/000136335
25. Hampton MB, Kettle AJ, Winterbourn CC. Inside the neutrophil phagosome: oxidants, myeloperoxidase, and bacterial killing. *Blood.* 1998;92(9):3007–3017. doi:10.1182/blood.V92.9.3007
26. Symington JW, Wang C, Twentyman J, et al. ATG16L1 deficiency in macrophages drives clearance of uropathogenic *E. Coli* in an IL-1 β -dependent manner. *Mucosal Immunol.* 2015;8(6):1388–1399. doi:10.1038/mi.2015.7
27. Russell DG, Huang L, VanderVen BC. Immunometabolism at the interface between macrophages and pathogens. *Nat Rev Immunol.* 2019;19(5):291–304. doi:10.1038/s41577-019-0124-9
28. Rohde K, Yates RM, Purdy GE, Russell DG. Mycobacterium tuberculosis and the environment within the phagosome. *Immunol Rev.* 2007;219(1):37–54. doi:10.1111/j.1600-065X.2007.00547.x
29. Veiga-Fernandes H, Artis D. Neuronal-immune system cross-talk in homeostasis. *Science.* 2018;359(6383):1465–1466. doi:10.1126/science.aap9598
30. Gabanyi I, Muller PA, Feighery L, et al. Neuro-immune interactions drive tissue programming in intestinal macrophages. *Cell.* 2016;164(3):378–391. doi:10.1016/j.cell.2015.12.023
31. Klose CSN, Mahlaköiv T, Moeller JB, et al. The neuropeptide neuromedin U stimulates innate lymphoid cells and type 2 inflammation. *Nature.* 2017;549(7671):282–286. doi:10.1038/nature23676
32. Brain SD, Williams TJ. Inflammatory oedema induced by synergism between calcitonin gene-related peptide (CGRP) and mediators of increased vascular permeability. *Br J Pharmacol.* 1985;86(4):855–860. doi:10.1111/j.1476-5381.1985.tb11107.x
33. Shi X, Wang L, Clark JD, Kingery WS. Keratinocytes express cytokines and nerve growth factor in response to neuropeptide activation of the ERK1/2 and JNK MAPK transcription pathways. *Regul Pept.* 2013;186:92–103. doi:10.1016/j.regpep.2013.08.001

34. Behzadi E, Behzadi P. The role of toll-like receptors (TLRs) in urinary tract infections (UTIs). *Cent European J Urol*. 2016;69(4):404–410. doi:10.5173/cej.2016.871
35. Behzadi P, García-Perdomo HA, Karpiński TM. Toll-like receptors: general molecular and structural biology. *J Immunol Res*. 2021;2021:9914854. doi:10.1155/2021/9914854
36. Bratton DL, Henson PM. Neutrophil clearance: when the party is over, clean-up begins. *Trends Immunol*. 2011;32(8):350–357. doi:10.1016/j.it.2011.04.009
37. Soehnlein O, Lindbom L. Phagocyte partnership during the onset and resolution of inflammation. *Nat Rev Immunol*. 2010;10(6):427–439. doi:10.1038/nri2779
38. Benoit M, Desnues B, Mege J. Macrophage polarization in bacterial infections. *J Immunol*. 2008;181(6):3733–3739. doi:10.4049/jimmunol.181.6.3733
39. Mehta A, Brewington R, Chatterji M, et al. Infection-induced modulation of m1 and m2 phenotypes in circulating monocytes: role in immune monitoring and early prognosis of sepsis. *Shock*. 2004;22(5):423–430. doi:10.1097/01.shk.0000142184.49976.0c
40. Bozza FA, Salluh JI, Japiassu AM, et al. Cytokine profiles as markers of disease severity in sepsis: a multiplex analysis. *Crit Care*. 2007;11(2):R49. doi:10.1186/cc5783
41. Chen F, Wu W, Millman A, et al. Neutrophils prime a long-lived effector macrophage phenotype that mediates accelerated helminth expulsion. *Nat Immunol*. 2014;15(10):938–946. doi:10.1038/ni.2984
42. Kolaczowska E, Kubes P. Neutrophil recruitment and function in health and inflammation. *Nat Rev Immunol*. 2013;13(3):159–175. doi:10.1038/nri3399
43. Abtin A, Jain R, Mitchell AJ, et al. Perivascular macrophages mediate neutrophil recruitment during bacterial skin infection. *Nat Immunol*. 2014;15(1):45–53. doi:10.1038/ni.2769
44. Buckley CD, Gilroy DW, Serhan CN, Stockinger B, Tak PP. The resolution of inflammation. *Nat Rev Immunol*. 2013;13(1):59–66. doi:10.1038/nri3362
45. Matak I, Lacković Z. Botulinum toxin A, brain and pain. *Prog Neurobiol*. 2014;119:39–59. doi:10.1016/j.pneurobio.2014.06.001
46. Grando SA, Zachary CB. The non-neuronal and nonmuscular effects of botulinum toxin: an opportunity for a deadly molecule to treat disease in the skin and beyond. *Br J Dermatol*. 2018;178(5):1011–1019. doi:10.1111/bjd.16080
47. Chermansky CJ, Chancellor MB. Use of botulinum toxin in urologic diseases. *Urology*. 2016;91:21–32. doi:10.1016/j.urology.2015.12.049
48. Giannantoni A, Mearini E, Del ZM, Proietti S, Porena M. Two-year efficacy and safety of botulinum toxin intravesical injections in patients affected by refractory painful bladder syndrome. *Curr Drug Deliv*. 2010;7(1):1–4. doi:10.2174/156720110790396463
49. Apostolidis A, Dasgupta P, Fowler CJ. Proposed mechanism for the efficacy of injected botulinum toxin in the treatment of human detrusor overactivity. *Eur Urol*. 2006;49(4):644–650. doi:10.1016/j.eururo.2005.12.010

Publish your work in this journal

The Journal of Inflammation Research is an international, peer-reviewed open-access journal that welcomes laboratory and clinical findings on the molecular basis, cell biology and pharmacology of inflammation including original research, reviews, symposium reports, hypothesis formation and commentaries on: acute/chronic inflammation; mediators of inflammation; cellular processes; molecular mechanisms; pharmacology and novel anti-inflammatory drugs; clinical conditions involving inflammation. The manuscript management system is completely online and includes a very quick and fair peer-review system. Visit <http://www.dovepress.com/testimonials.php> to read real quotes from published authors.

Submit your manuscript here: <https://www.dovepress.com/journal-of-inflammation-research-journal>